



## Short communication

## Fabrication and characterization of a micro-fuel cell made of metallized PMMA

J.A. Alanís-Navarro<sup>a</sup>, C. Reyes-Betanzo<sup>b</sup>, J. Moreira<sup>c</sup>, P.J. Sebastian<sup>a,\*</sup><sup>a</sup> Instituto de Energías Renovables-UNAM, Temixco, Morelos, 62580, México<sup>b</sup> Instituto Nacional de Astrofísica, Óptica y Electrónica, Luis Enrique Erro 1, Tonantzintla Puebla, 72840, México<sup>c</sup> DES de Ingeniería, Universidad de Ciencias y Artes de Chiapas, Libramiento Norte Poniente, 29039, Tuxtla Gutiérrez, Chiapas, México

## HIGHLIGHTS

- A micro fuel cell was fabricated with PMMA as the base material.
- Cu, Mo and Au multilayers on PMMA were characterized.
- Physico-chemical and electrochemical studies were done on the micro-fuel cell.
- Metal coating adhesion was enhanced by thermal treatment.

## ARTICLE INFO

## Article history:

Received 3 January 2013

Received in revised form

4 May 2013

Accepted 13 May 2013

Available online 20 May 2013

## Keywords:

Micro-fuel cell

PMMA

Hydrogen

Monopolar plate

## ABSTRACT

In this work we propose the fabrication and characterization of a micro-fuel cell prototype based on the low mass density polymer poly(methyl-methacrylate) (PMMA), having low aspect ratio micro-channels, which were superficially metallized via sputter deposition technique. For current collector and anti-corrosion coatings we employed different high electrical conductivity materials such as copper, molybdenum and gold. Metallic coatings were physically and chemically characterized by using scanning electron microscopy for the topographical analysis, X-ray diffraction for the structural analysis and energy dispersive spectroscopy for composition analysis. The electrical and electrochemical parameters obtained for the prototype cell were: a mean open circuit potential of 855 mV, a maximum electrical power density of  $73 \mu\text{W cm}^{-2}$  at  $182 \mu\text{A cm}^{-2}$  and 380 mV.

© 2013 Elsevier B.V. All rights reserved.

## 1. Introduction

The ever-growing electronic device market requires high specific energy and energy density fuels and materials for energy conversion and storage. Micro or miniature fuel cells have a great potential as energy sources for low power applications, mainly in wireless telecommunications, information technology and for micro-power generation, as a sustainable alternative to secondary batteries. Low power applications include portable electronic devices like PDAs, mobile phones, digital cameras and electronic toys. According to the mobility requirements, the fuel sources can be either gaseous or liquid and even solid ones like metal hydrides.

In fuel cells, as in other energy storage and energy conversion systems, the chosen fuel is crucial in their performance. In the

energy conversion and storage systems, specific energy and energy density of fuels play an important role in the overall performance. It is expected that the fuel has great energy content per unit mass and per unit volume. Fig. 1 shows the specific energy of different fuels normalized to the Lithium-ion specific energy value. It is possible to observe that hydrogen has the highest value. The prospect of micro-fuel cells replacing batteries in mobile devices is considered in terms of their high specific energy and energy density, technological feasibility, low cost and low weight of devices [2]. Currently, micro-fuel cell technology seems to be a great candidate to replace secondary ion batteries based on Lithium-ion material [3–5]. Therefore, high specific energy fuels must be employed for helping to mitigate the main problems associated with energy storage capacity, and also to be in a straightforward manner, an environmentally friendly alternative to the pollutant secondary batteries. In Ref. [2,6] the authors show the feasibility to produce electrical power through micro-solid oxide fuel cell, however this type of FC still needs a prohibitive temperature (up to 750 °C) for portable

\* Corresponding author.

E-mail addresses: [sjp@ier.unam.mx](mailto:sjp@ier.unam.mx), [sjp@cie.unam.mx](mailto:sjp@cie.unam.mx) (P.J. Sebastian).

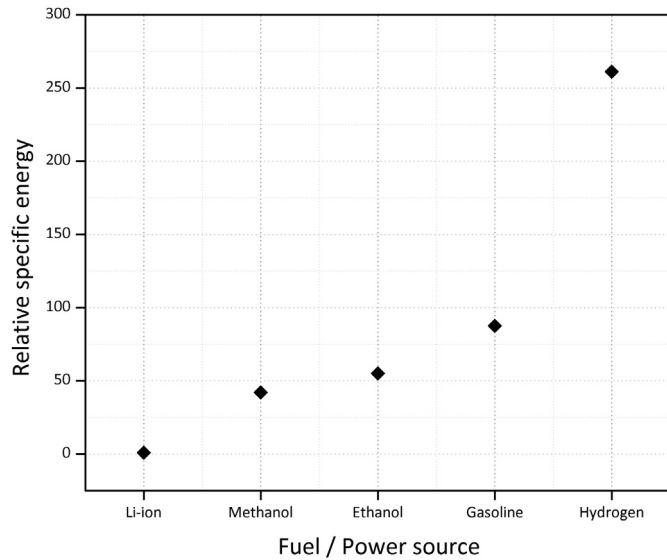


Fig. 1. Specific energies of different fuels/power sources and materials for energy storage. Data extracted from Ref. [1].

applications. In this work, it is proposed to develop and characterize a micro-fuel cell prototype for low power applications, which is made of metallized polymer poly(methyl-methacrylate). Certainly we chose this material because of its low mass density, however it is important to remember that PMMA is an economic material. As you see, in our design the PMMA serves as a mechanical support and for mechanize the flow fields, which substitutes to graphite in conventional cells. The metal coatings provide the electrical and thermal conductivity characteristics for an appropriate performance.

The goal of this work is to construct and characterize the prototype at a laboratory scale. Even though the current and power density values are lower compared to the other micro-fuel cells already reported, it is one of the first attempts to utilize a PMMA polymer as current collector plate in this type of fuel cells.

## 2. Materials and methods

### 2.1. Design considerations

When the physical dimensions of devices are reduced, all phenomena related to the volume, body forces, e.g., gravity and electromagnetic forces can be neglected. On the other hand, other kinds of phenomena greatly predominate, i.e., surface effects such as surface tension and capillarity effects. As a consequence, at the micro-scale, viscous forces play an important role, even more than inertial ones [7], and it will be included as design criteria. In some micro-fluidic devices using micro-channels, typical assumptions of continuum fluid mechanics cannot be directly made. Laminar flow regime in  $\mu$ FCs is below 400 Reynolds number instead of 2300 in meso or macroscopic approaches [8]. To establish the approach that it must be used, Fig. 2 shows the calculated Knudsen number as a function of hydraulic diameter ( $D_h$ ) of micro-channels, ranging from 100 nm to 600  $\mu$ m. The Knudsen number is expressed as the ratio of the mean free path ( $\lambda$ ) of the molecules to the characteristic length ( $L$ ) of the system, see Eq. (1). For non-cylindrical pipes  $L$  is generally equal to the hydraulic diameter [9] and  $\gamma$  is the specific heat ratio.  $Ma$  and  $Re$  are the dimensionless parameters, Mach number and Reynolds number respectively. For most gases the non-slip flow regime breaks down at  $Kn < 1 \times 10^{-3}$ , this limit is

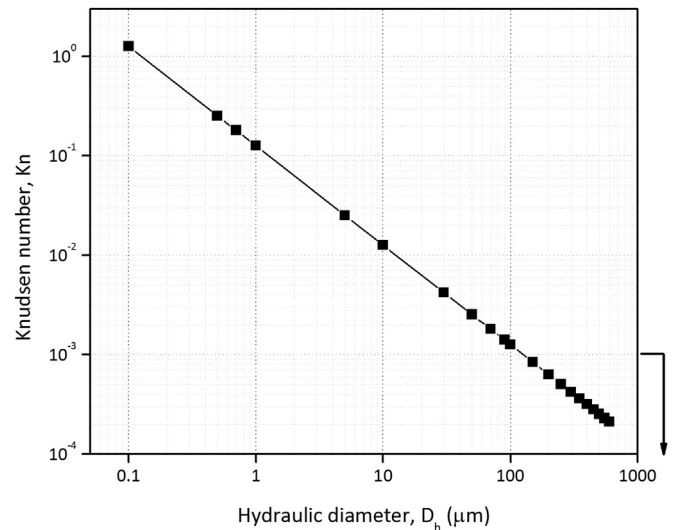


Fig. 2. Logarithmic plot of Knudsen number as a function of hydraulic diameter of micro-channels.

defined by the arrow in Fig. 2. The proposed design lies in the non-slip flow regime, then no other consideration as rarefaction effects must be regarded.

$$k_n = \frac{\lambda}{L} = \frac{Ma}{Re} \sqrt{\frac{\pi\gamma}{2}} \quad (1)$$

### 2.2. Flow field design

A great variety of flow fields have been designed to improve the heat and electrical charge management, also for uniform gas distribution and minimize the pressure drop. Fig. 3 shows the typical designs, namely: a) single serpentine, b) parallel, c) multiple serpentine, and d) grid type flow fields. A channel to rib ratio (CR) of

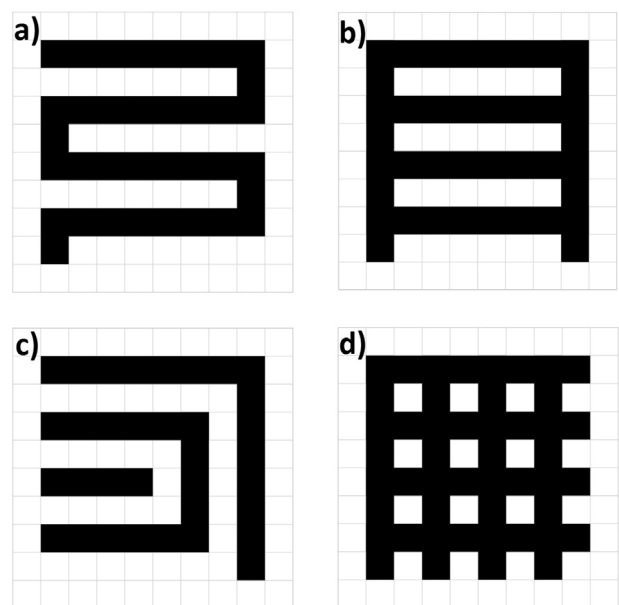


Fig. 3. Partial top view of different flow field configurations with a CR = 1: a) single serpentine, b) parallel, c) multiple serpentine and d) grid type. The fluid flows through the black path.

unity was chosen for comparison purposes. In this qualitative analysis, the aspect ratio (AR) of micro-channels was not regarded. If a dielectric supporting material was chosen as the raw material for machining the flow field, the electronic conduction would be restricted to be essentially superficial, not through the bulk, as it normally happens. Focusing on this idea, the rib area alone is used for electronic conduction, hence the contact area predominates. This issue will be addressed in the next section.

2.2.1. Geometrical and electrical constraints

In micro-fuel cells the concept of bipolar plates does not make sense, hence mono-polar and planar approaches must be adopted. If a dielectric material has been chosen as the supporting material for the flow field, the electrical contact area is an issue, and it must be maximized without sacrificing the flow paths for fuel and oxidant flows. In Fig. 4 it is shown the calculated percentage area, which is considered as the path for electronic conduction. This is the case if a dielectric material is used for machining the flow field plates. Additionally, the interconnection between  $\mu$ FCs made of dielectric materials must be in a side-by-side configuration [10]. Fig. 5 shows an isometric partial view of a single serpentine flow field type design; the channels have a semicircular cross-sectional area. Although this flow field pattern is considered as the simplest, it plays an important role in commercial FCs. At the right bottom hand of the same figure the dimensionless CR and AR design parameters are defined.

2.3. Proposed design

The physical characteristics of the proposed design are briefly described. To achieve uniform pressure over the entire flow field, a PMMA substrate thickness of 3 mm was chosen, this thickness avoids substrate bending. The flow field geometrical area is  $1 \text{ cm}^2$ ; a single serpentine flow field was chosen to maximize the electronic conduction area, as it was justified through Fig. 4. In order to compensate both the heat transfer and the fluid flow through the micro-channels, the channel to rib ratio of unity, i.e.,  $CR = 1$ , was selected. The aspect ratio is one half,  $AR = 1:2$ , the micro-channels are  $300 \mu\text{m}$  wide and  $150 \mu\text{m}$  deep; the cross-sectional shape of micro-channels is rectangular. Two  $0.8 \text{ mm}$  diameter holes were made as inlet–outlet ports for fuel and oxidant flows were done.

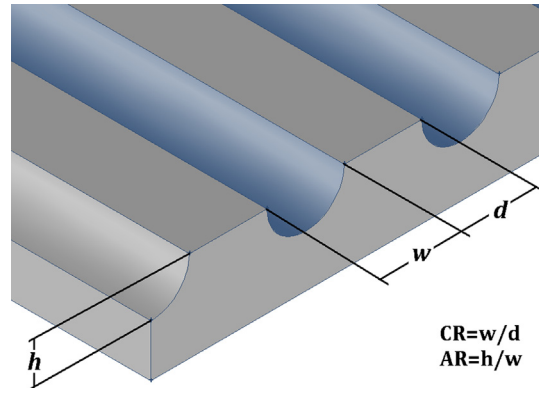


Fig. 5. Isometric view of a single serpentine type flow field. Dimensionless CR and AR design parameters are defined.

The hydraulic connections were made via commercial syringes. After the flow field has been machined, the PMMA surface was coated using different metal thin films deposited via a low temperature deposition technology, the direct current sputtering technique. The membrane–electrode–assembly was made based on the state-of-the-art technique: a  $0.5 \text{ mg cm}^{-2}$  catalyst loading based on pure platinum supported on carbon; thin Teflon<sup>®</sup> treated and untreated carbon paper was used as gas diffusion layers for cathode and anode zones respectively; the membrane used was a Nafion<sup>®</sup> 115 and commercial silicon gaskets were used as separators.

3. Results and discussion

3.1. Fabrication of the micro-fuel cell

The earlier micro-fuel cell prototypes were a miniature replica of the conventional heavy fuel cells, using graphite as the structural material for the fabrication of flow field plates and commercial membrane–electrode assemblies. Later on, when the research and development have acquired a reasonable maturity, materials used

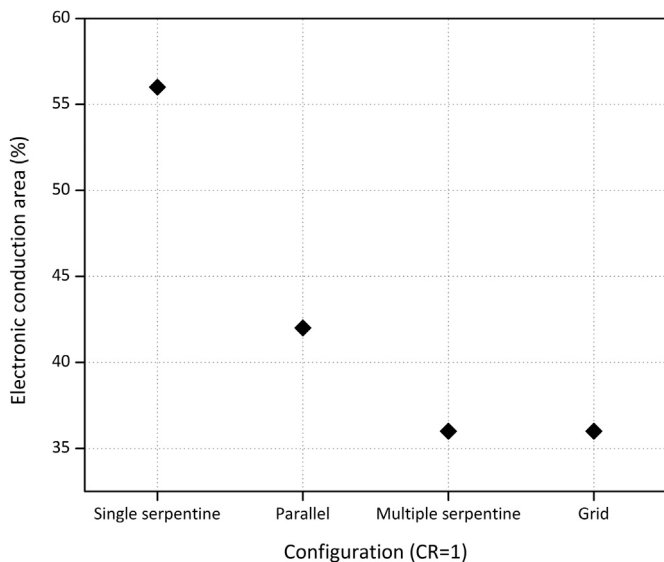


Fig. 4. Calculated area for electronic conduction of different flow fields.

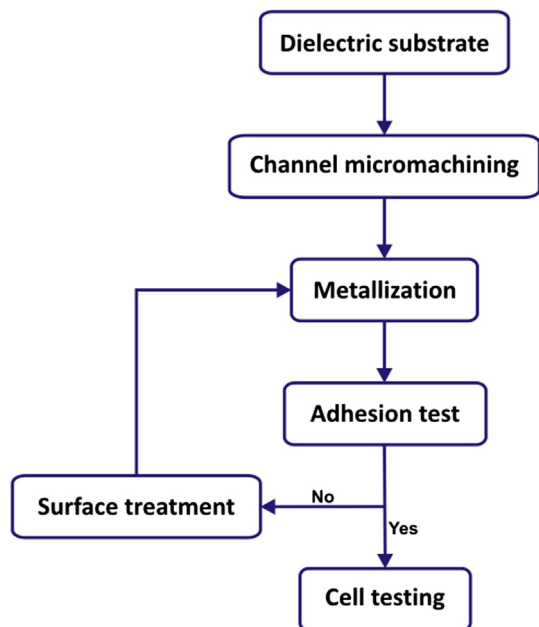


Fig. 6. Complete fabrication process flux diagram.



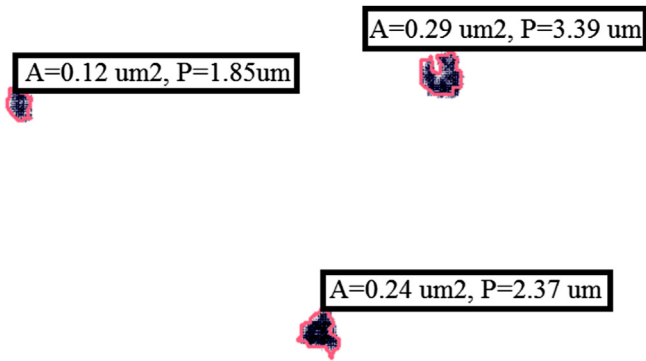


Fig. 7. Partial view of a thermally treated molybdenum thin film subjected to the adhesion test.

in the semiconductor industry predominated as the base materials for if prototypes: crystalline silicon, metals, borofloat glasses, and materials as thin films physically or chemically deposited over the substrates. However, in order to reach pre-commercial devices, recently there is an increase in the use of new materials based on polymers, both organics and inorganics, due to their lightweight and low cost advantages. In this work, the cheaper polymer, poly(methyl methacrylate) was used as the mono-polar plates, the micro-channels were mechanized via a rapid prototype tool (ProtoMat C40 by Lasser Electronics company). For current collectors and anti-corrosion coatings, different metals were explored. The overall fabrication processes is schematized in Fig. 6 through the flux diagram.

### 3.2. Metallization

It is well known that the adherence of metals to polymers is an issue, especially to poly(methyl-methacrylate), (PMMA), but it could be overcome via surface pre-treatments. This surface

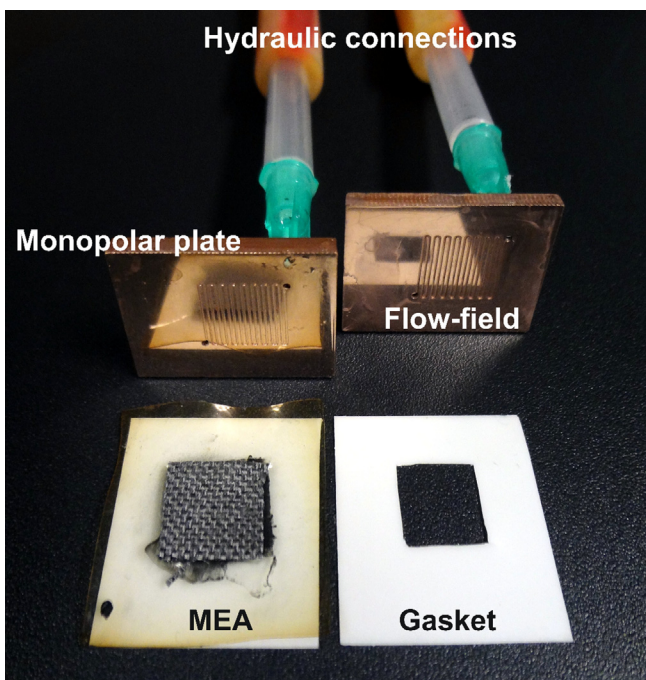


Fig. 8. Copper metallized PMMA micro-fuel cell prototype.

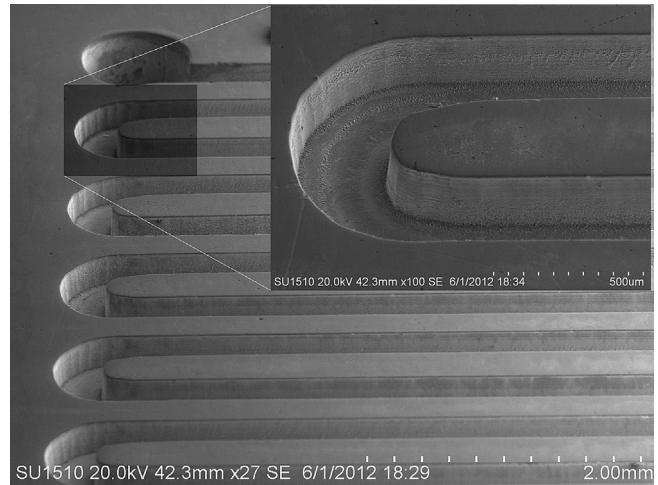


Fig. 9. SEM picture of micro-channels fabricated on PMMA polymer forming the flow field.

modification can be mechanical, chemical or even plasma assisted [11]. These methods serve for slightly roughening the surface; this helps to increase the anchor points, and to improve the chemical bonding between two materials. In this work, the chemical surface treatments comprise treatments either in diluted or concentrated acids and alkaline solutions in different concentrations. Both acid and alkaline solutions were selected based on the degree of chemical interaction between the substrate and solvents. Plasma treatment involves low-density plasma created by a direct current plasma system, using argon, oxygen and their mixture. To evaluate the adhesion enhancement, a simplified version of the cross-cut-test was implemented. This step is explained below. In order to collect the electric current and to create an anti-corrosion coating, different materials were explored: i) copper, ii) molybdenum, iii) gold, iv) titanium and v) indium–tin oxide (ITO). The last two materials deposited as thin films via the DC sputtering are too electrically resistive for the proposed application, their properties do not reach the bulk properties, the very slow deposition rate generates resistive very thin films. On the other hand, copper, molybdenum and gold work well. Different multilayer schemes were studied: i) PMMA/Cu, ii) PMMA/Cu/Au, iii) PMMA/Cu/Mo, and finally iv) PMMA/Cu/Mo/Au scheme.

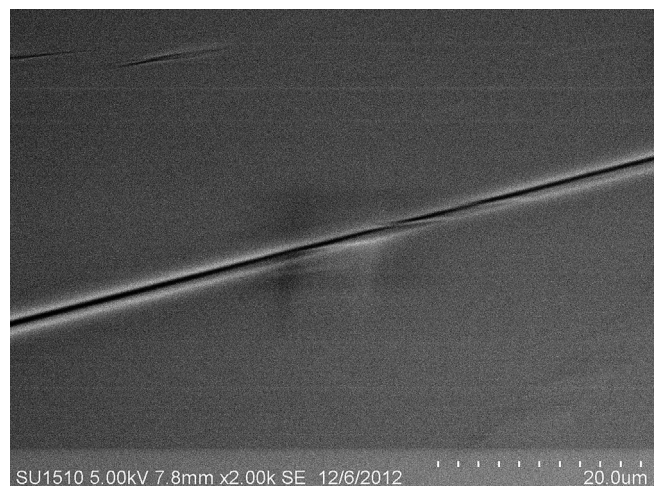


Fig. 10. Representative SEM picture of Cu/Mo/Au coated PMMA substrate: a magnification of 20,000 was used.

3.2.1. Adhesion test

In order to quantify the adherence of metals to PMMA, a simplified version of the cross-cut test [12] was implemented. In this work, this proof was implemented as follows: an adhesive stripe was stuck onto the metal film surface; then it was pulled off perpendicularly with respect to the surface. If the thin film remains over the substrate, it is considered that the film has good adhesion strength, if not the film lacks of good adhesion. Using this simplified version of the cross-cut-test it is possible to evaluate the thin film's capability to adhere over the substrates. It is possible to use this proof as a qualitative and/or quantitative measure of thin film adhesion strength as a binary measure: whether it can adhere or not, or expressed as an area percentage of the un-removed film. All measurements made over the chemically and mechanically treated substrates were unfavorable. The plasma treatment of argon, oxygen and their mixture showed inconsistent results. However, the samples subjected to the thermal treatment presented better results, showing an area percentage of un-removed film below 2%. The thermal treatment was made with a convection heat oven during different exposure times and temperature gradients. The optimum thermal treatment conditions are: near PMMA's glass transition temperature, *i.e.*,  $115 \pm 3 \text{ }^\circ\text{C}$  for 1.5 h. Thermal treatments made below this period do not have any adhesion enhancement. In Fig. 7 it is shown a representative image used to measure the thin

film's adhesion quality via a simplified version of cross-cut-test. This figure corresponds to a molybdenum thin film (the white zone), the removed film is evident through the black zones. After this adherence enhancement study was completed, the micro-fuel cell fabricated was analyzed. In Fig. 8 it is shown the fabricated micro-fuel cell prototype, its mass is around 3.8 g, including the mono-polar plates, the MEA and gaskets. In Fig. 9 it is shown a close up of micro-channels.

3.3. Physical and chemical characterization

The physical characterization consisted of a topographic qualitative analysis via scanning electron microscopy. In this study a SEM Hitachi SU1510 was used. In this characterization step, it was possible to observe qualitatively a very low roughness thin film because of the smooth PMMA substrate surface; therefore all the subsequent metallic coatings were deposited in a conformal way. Because of the topographical similarity of the different layers, only a representative image of the surface thin film is shown. This picture corresponds to the top film of the PMMA/Cu/Mo/Au multilayer configuration, see Fig. 10. A surface defect was used to focus the film surface. It is expected that this very low roughness significantly contributes to the decrease of the overall electrical contact resistance, and hence improving the electrical power density.

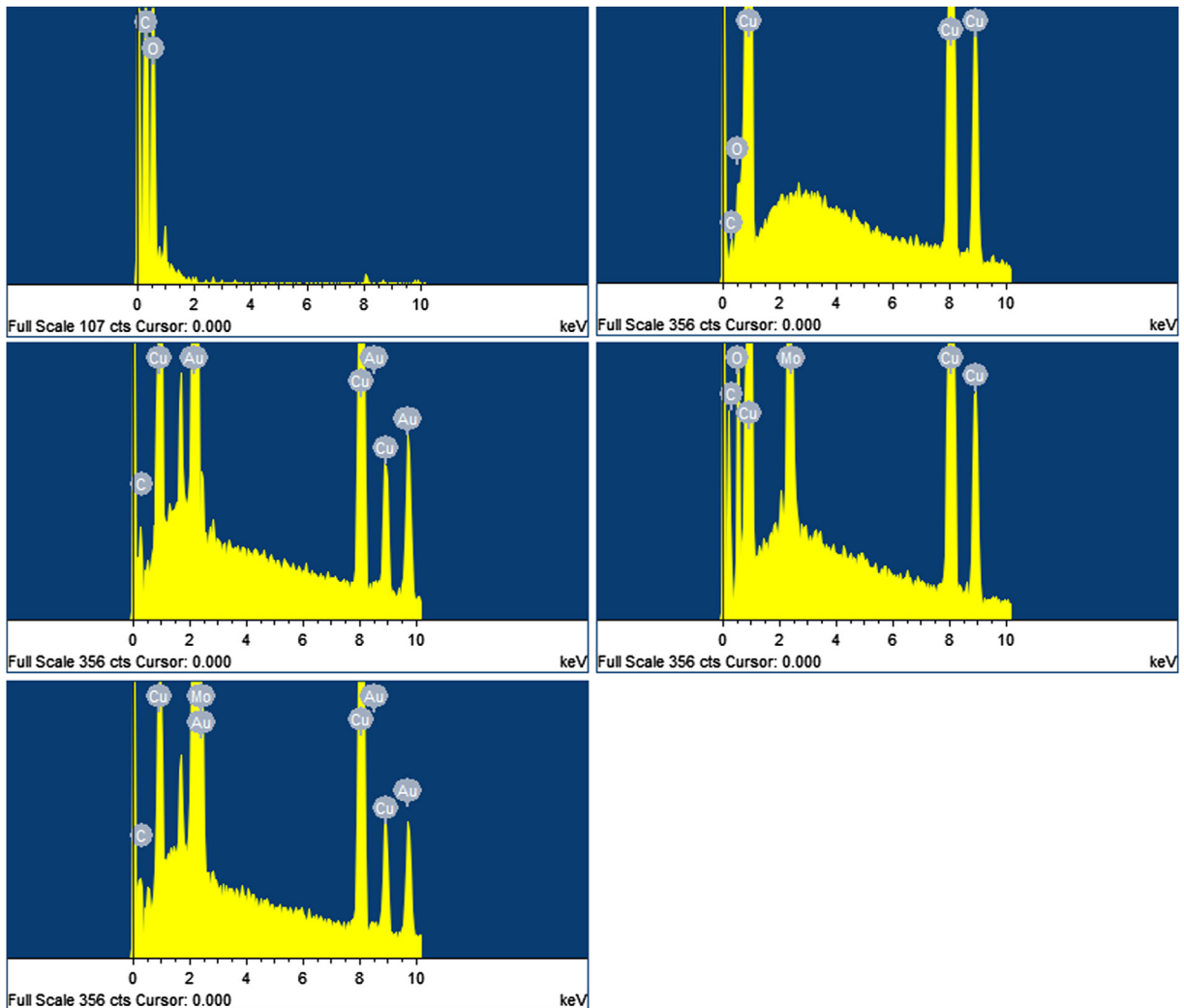


Fig. 11. Energy-dispersive X-ray results: top-left PMMA; top-right PMMA/Cu; middle-left PMMA/Cu/Au; middle-right PMMA/Cu/Mo; bottom-left PMMA/Cu/Mo/Au.

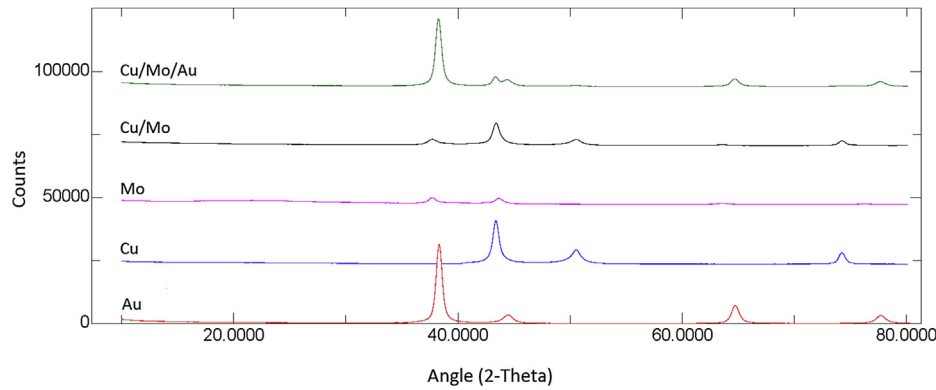


Fig. 12. X-ray diffraction measurements showing the main peaks of different metallic multilayer configuration.

The chemical characterizations consisted of Energy-Dispersive X-Ray Spectroscopy (EDS or EDX) and X-Ray Diffraction (XRD) measurements of the complete multilayer configurations. The EDS analysis was made using a SEM Hitachi SU1510 having an X-ray detector. The energy peaks are shown in Fig. 11. It is possible to observe the characteristic peaks of each material, corresponding to the  $K\alpha$ ,  $L\alpha$  and  $M\alpha$  energy emission lines. All the samples were analyzed by using X-ray diffraction equipment, the DMAX 2200 model by Rigaku company. The XRD analysis consisted of small angle measurements, the 2.5–40 degrees range was used, see Fig. 12. The XRD patterns for the different configurations of metallic layers show peaks corresponding to Cu, Mo and Au.

### 3.4. Electrical characterization

The electrical characterization of the prototype micro fuel cell was done with an ElectroChem fuel cell Test Station (MTS-150) for gas supply, an Electronic Cell Load (ECL-150) for electrical current and electrical potential measurements. Polarization curves were obtained at standard temperature and pressure conditions. Volumetric flow gases were symmetrically supplied at both the cathode and the anode zones: 25 and 30 ml  $\text{min}^{-1}$ . In Fig. 13 it is shown the experimental results. It is possible to distinguish all the zones existing in a typical fuel cell: activation, ohmic and diffusion losses. The electrical and electrochemical parameters obtained for the prototype cell were: a mean open circuit potential of 855 mV, a maximum electrical power density of 73  $\mu\text{W cm}^{-2}$  at 182  $\mu\text{A cm}^{-2}$  and 380 mV. The electrical current density and electrical power

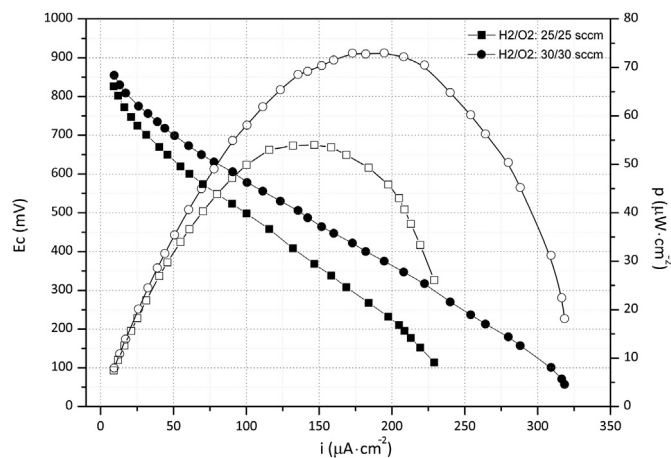


Fig. 13. Electrical potential and electrical power density as a function of electrical current density.

density of our micro-fuel cell prototype do not reach those of the actual state-of-the-art micro-fuel cells. We lack of a standardized membrane-electrode-assembly manufacturing processes, however we are working to improve the electrical performance of the prototype.

### 4. Conclusions

A micro-fuel cell prototype was designed and manufactured using cheap and low mass density materials. The copper adhesion was enhanced via a thermal treatment and no hazardous materials were employed. The micro-fuel cell prototype based on the low mass density polymer poly(methyl-methacrylate) having low aspect ratio micro-channels was superficially metallized. The figure of merit showed an open circuit electrical potential of 855 mV, using very low volumetric flow rates, a maximum electrical power density of 73  $\mu\text{W cm}^{-2}$  at 182  $\mu\text{A cm}^{-2}$  and 380 mV. Even though these preliminary results differ from the previous work reported [13], it is expected to greatly enhance the performance by means of an improved MEA manufacturing process.

### Acknowledgments

The authors acknowledge the technical assistance received from Mr. Gildardo Casarrubias, Mr. Abraham Torres, Mr. José Campos, Ms. María Luisa Ramón and Ms. Patricia Altúzar. This work was carried out as part of the projects IN 103410 and CONACYT 100212.

### References

- [1] D. Lide, Handbook of Chemistry and Physics, 87th ed., CRC Press, Colorado, USA, 2007.
- [2] J. Rupp, A. Gauckler, A. Evans, Hutter, Journal of Power Sources 194 (2009) 119–129.
- [3] G. Reddy, Y. Lu, Journal of Power Sources 195 (2010) 503–508.
- [4] N. Hashim, S.K. Kamarudin, W.R.W. Daud, International Journal of Hydrogen Energy 34 (2009) 8263–8269.
- [5] S. Giddey, S.P.S. Badwal, F.T. Ciacchi, D. Fini, B.A. Sexton, F. Glenn, P.W. Leech, International Journal of Hydrogen Energy 35 (2010) 2506–2516.
- [6] N. Akhtar, S.P. Decent, D. Loghini, K. Kendall, Journal of Power Sources 193 (2009) 39–48.
- [7] M. Gad el Hak, Mems Handbook, CRC Press, Richmond, USA, 2006.
- [8] H. Bruus, Theoretical Microfluidics, Oxford University, New York, USA, 2008.
- [9] L. Vasiliev, S. Kakac, A. Pramuanjarokij, Mini-micro Fuel Cells: Fundamentals and Applications, Springer, Dordrecht, The Netherlands, 2007.
- [10] S.W. Cha, R. O'Hayre, Y.L. Park, Y. Saito, F.B. Prinz, S.J. Lee, A. Chang-Chien, Journal of Power Sources 112 (2002) 410–418.
- [11] K. De Bruyn, M. Van Stappen, H. De Deurwaerder, L. Rouxhet, J.P. Celis, Surface & Coating Technology 163–164 (2003) 710–715.
- [12] Standard Test Methods for Measuring Adhesion by Tape Test (2012). www.techstreet.com. Technical report, ASTM D3359.
- [13] T.S. Zhao, Micro Fuel Cells Principles and Applications, Academic Press, Burlington, USA, 2009.